RSC Sustainability

ROYAL SOCIETY OF CHEMISTRY

PAPER

View Article Online
View Journal | View Issue

Cite this: *RSC Sustainability*, 2023, **1**, 511

Super-fast iodine capture by an ionic covalent organic network (iCON) from aqueous and vapor media†

Prince, Atikur Hassan, Sohom Chandra, Akhtar Alam and Neeladri Das *

Global concerns related to the rise in worldwide energy demand, along with the pledge to minimize greenhouse gas emissions, have encouraged developed nations to opt for clean, efficient, and sustainable nuclear energy. However, the generation of volatile radioactive by-products (such as ^{129}I and ^{131}I) during the operation of a nuclear power plant is considered a serious environmental concern, especially in the case of an accident. As a result, the development of efficient iodine sequestering adsorbents from both aqueous and vapor media is an important contemporary research domain. In this regard, we report herein a guanidinium-based ionic covalent organic network (iCON), denoted as iCON-4, that was prepared using a Schiff-base polycondensation reaction between terephthalaldehyde and triaminoguanidinium chloride. The polymeric iCON-4 is robust and it exhibits good physiochemical stability. The positively charged guanidinium moieties present in iCON-4 facilitate the ion-exchange based adsorption of iodine leading to faster uptake kinetics as well as relatively higher capture capacity. In fact, the iCON-4 polymeric network shows iodine removal greater than 99% from the aqueous medium within two minutes and it shows excellent affinity (distribution coefficient, ~10^5 ml g^{-1}) towards iodine in the aqueous medium. Also, it displays fast kinetics during the removal of iodine species from aqueous water samples collected from diverse water bodies such as seas, rivers and lakes. Additionally, iCON-4 registered remarkable selectivity while capturing iodide ions in the presence of other competing anionic species. For practical applications, iCON-4 can be reused up to seven times without any remarkable loss in uptake performance. Thus, iCON-4 has been developed as a strategic material with all desirable attributes required in an adsorbent for practical applications.

Received 3rd December 2022
Accepted 23rd February 2023

DOI: 10.1039/d2su00117a

rsc.li/rscsus

Sustainability spotlight

With the growing need for the establishment of clean energy sources with negligible greenhouse gas emissions, a closer look at nuclear energy is required. Although nuclear energy is one of the most low-carbon energy sources, the simultaneous accumulation of nuclear waste and its accidental leakage into water bodies and the atmosphere pose a serious concern. Moreover, the presence of certain isotopes of volatile iodine (^{129}I and ^{131}I) in nuclear waste is a significant concern due to their radiotoxicity and mobility. Therefore, it is of utmost importance to develop materials for efficiently trapping iodine species. In this context, a relatively 'greener approach' was employed to synthesize a guanidium-based ionic covalent organic network (iCON-4) containing an imine linkage. Additionally, iCON-4 can be reused several times for removing iodine from real-time water samples. Furthermore, the present work is aligned with goal 6 of "Clean Water and Sanitation," goal 7 of "Affordable and Clean Energy," and goal 13 of "Responsible Consumption and Production" in the UN's Sustainable Development Goals.

Introduction

Harnessing nuclear energy is becoming a preferred alternative to the use of fossil fuels in order to meet the ever-increasing global energy demands.[1,2] Additionally, commercial nuclear power plants also aid in checking atmospheric CO_2 (a greenhouse gas) emissions and associated environmental issues of global warming and ocean acidifications.[3] Efficient processing of spent nuclear fuel is essential to reduce the quanta of hazardous 'high-level' radioactive wastes and recover fissile materials for their reuse as fuel.[4–6] During nuclear waste management, handling of volatile and radioactive fission waste such as ^{129}I requires the use of efficient adsorbents at the source.[7,8] ^{129}I is a concern because of its rather long half-life (>10^7 years), high mobility and tendency to biomagnify.[9] ^{129}I emits β-particles along with high energy γ- and X-rays.[10] Another radioisotope of iodine ^{131}I has medicinal applications such as treatment of hyperthyroidism and thyroid cancer.[11–13] However, accidental exposure to ^{131}I and its accumulation in thyroid

Department of Chemistry, Indian Institute of Technology Patna, Patna 801106, Bihar, India. E-mail: neeladri@iitp.ac.in; neeladri2002@yahoo.co.in; Tel: +91 9631624708

† Electronic supplementary information (ESI) available. See DOI: https://doi.org/10.1039/d2su00117a

glands of a healthy individual may lead to serious health complications.[14,15] In fact, the unfortunate Chernobyl nuclear power plant accident in the last century exposed Ukrainian citizens to significant quantities of ^{131}I.[16–18] Iodine is frequently used to disinfect water, although leftover iodine and iodide must be removed for health concerns.[19–21] Considering these facts, there is a necessity to develop novel adsorbents for efficient capture as well as storage of molecular iodine.[22,23] In other words, finding effective ways to successfully capture and store volatile radioactive iodine is critical for both public and nuclear safety.[24] In recent past, the sequestration of iodine using physical, biological, and chemical techniques has received a lot of attention.[2,25–31] Such studies utilize the non-radioactive and naturally available isotope of iodine (^{127}I) as a surrogate for radioiodine isotopes (^{129}I and ^{131}I).[4,32] Presently, silver-based composite adsorbents derived from zeolites are often used.[33,34] However, such materials are expensive and are associated with poor recyclability and low iodine adsorption capacities.[35] Other potential iodine adsorbents such as activated carbons and clays have limited surface areas and poor interactions with molecular iodine.[7,33] Thus, advanced porous materials such as metal–organic frameworks (MOFs), covalent organic frameworks (COFs), and porous organic polymers (POPs) are currently being studied extensively as porous materials for iodine capture and storage applications.[7,36–42]

POPs include materials with a multidimensional porous network obtained using organic monomers joined together by strong covalent linkages.[43–45] POPs are an exciting class of porous materials featuring low skeletal densities, superior thermal and chemical stabilities, high surface areas, and tuneable porous properties, making them one of the most promising options as adsorbents for iodine adsorption.[46–49] While there are a few reports of iodine capture by imine functionalized COFs/POPs, a literature survey indicates that the incorporation of ionic functionality is an important criterion for superior iodine capture by POPs.[50–53] While several materials have been reported for the capture/storage of both volatile radioiodine and iodine contained in organic solvents (such as hexane and methanol), there are only a handful of reports describing the removal of iodine species from aqueous solutions.[7,23] Humans remain at a risk of radioiodine exposure *via* consumption of agricultural produce cultivated with $^{129}I/^{131}I$ contaminated water. Thus, decontamination of water bodies polluted with radioactive iodine needs be addressed. In general, there is a need to develop ionic adsorbents that can capture iodine present in both vapor phase and aqueous media.

The current research thrust is towards the design of functional materials with fast and efficient radioiodine removal capabilities. In this context, ionic covalent organic networks are an emerging class of functional materials that are deliberately incorporated with ionic interfaces for inducing strong and attractive interactions with oppositely charged species.[54–60] Herein, we report the design and synthesis of an ionic covalent organic network (iCON-4) decorated with ionic functionalities and imine linkages for superior interaction with iodine. A Schiff-base polycondensation reaction was applied to obtain iCON-4 without using any acid or metal catalyst. iCON-4 was thoroughly characterized using various techniques and subsequently tested as an adsorbent for iodine present in the aqueous medium or vapor phase. The polymeric framework of iCON-4 contains guanidinium units that are essentially positively charged analogues of urea.[61] The guanidinium units form ion pairs with chloride ions.[62,63] It was anticipated that the weakly interacting chloride ions would be exchanged with iodide anions in our quest to obtain a new adsorbent with superior iodine capture kinetics and capacity.[62,64,65] Experimental results, described in the ensuing sections, indicate that the iodine capture capacity of iCON-4 from both aqueous and vapor phases is better than that of other previously reported ionic porous organic polymers or porous materials.

Experimental section

Materials

Terephthalaldehyde, guanidine hydrochloride, potassium iodide, iodine and hydrazine hydrate were purchased from Sigma Aldrich and Merck depending upon the availability. All other chemicals and reagents were procured locally and were used without any further purification. All the capture experiments were conducted with distilled water, unless otherwise stated. Real-time water samples (such as water from rivers and lakes) were obtained from the industrial and rural parts of Patna and Kolkata, India. In addition, a sea-water sample was collected from Juhu beach, Mumbai, India. Iodine stock solution was prepared by dissolving weighed quantities of KI and I_2 into distilled water.

Synthesis of triaminoguanidinium chloride (TAG_{Cl})

Triaminoguanidinium chloride was synthesized following a previously reported literature protocol.[66] Moreover, the detailed synthetic process is described on the page no. S-3 of the ESI.†

Synthesis of iCON-4

The polymeric network (iCON-4) was synthesized *via* a Schiff base reaction (Scheme 1) using triaminoguanidinium chloride (TAG_{Cl}) and terephthalaldehyde (TP) as monomers. Firstly, 0.3 mmol (40.24 mg) of TP and 0.2 mmol (28.12 mg) of TAG_{Cl} were taken in a Pyrex tube. Subsequently, the solid mixture was mixed with a solution of dioxane and water (2 : 0.6) and the contents of the Pyrex tube were sonicated for 15 minutes. The tube was then sealed and kept inside an oven for three days at 120 °C. After three days, iCON-4 was obtained as a bright yellow precipitate.

Capture studies

The polymeric network (iCON-4) was used to capture polyiodide ions from the aqueous solution. Initially, 0.25 mM iodine solution was prepared and tested for kinetics studies.

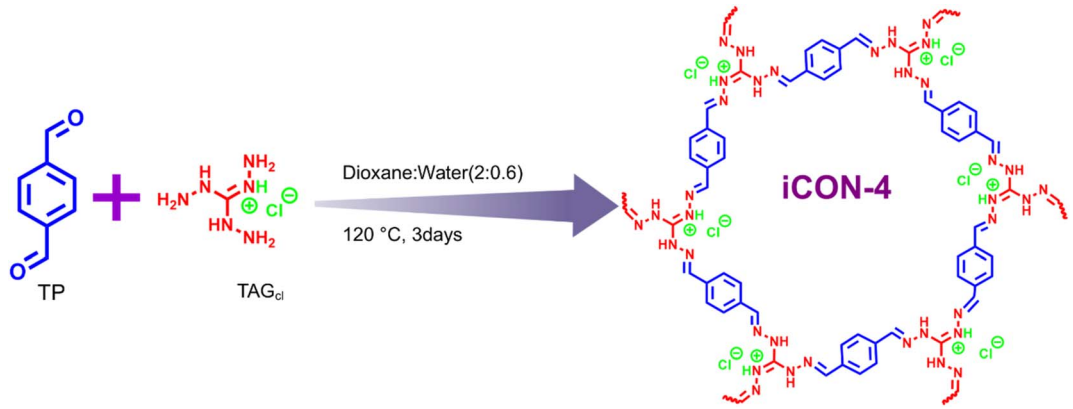

Scheme 1 Synthesis of iCON-4.

Kinetic studies

Time dependent experiments related to the removal of polyiodide ions from water were performed by UV-vis spectroscopy. Firstly, a stock solution of iodine was prepared and its absorbance was recorded. Subsequently, iCON-4 was added to the iodine solution with steady stirring. Later, the stirring was stopped to let the insoluble polymer settle down. Subsequently, the UV-visible spectrum of the supernatant liquid was recorded. From the obtained data, we have calculated the percentage removal of the polyiodide ions using eqn (1)

$$\%\ \text{removal} = \frac{C_0 - C_t}{C_0} \times 100. \quad (1)$$

where C_0 (mM) is the initial concentration and C_t (mM) is the final concentration of iodide ions at any given time t.

The kinetic data were fitted linearly according to pseudo-first order [eqn (2)] and pseudo-second order [eqn (3)] models. The expressions for both the models are represented in eqn (2) and (3) respectively.

$$\ln(Q_e - Q_t) = \ln Q_e - k_1 t \quad (2)$$

$$\frac{t}{Q_t} = \frac{1}{k_2 Q_e^2} + \frac{1}{Q_e} t \quad (3)$$

where Q_t (mg g^{-1}) and Q_e (mg g^{-1}) are the amounts of sorbate captured by iCON-4 at different time intervals (t) and at equilibrium respectively. Herein, t represents the time in seconds, and k_1 (sec^{-1}) and k_2 (g mg^{-1} s^{-1}) are the rate constants for pseudo first-order and pseudo-second order reactions, respectively.

Uptake capacity studies

10 mg of iCON-4 was added to iodine solution of known concentrations (0.25 to 10 mM) and stirred for three hours. Next, the solutions were filtered and the collected supernatant liquid was analysed *via* UV-vis spectroscopy. The collected data were fitted into Langmuir and Freundlich adsorption isotherm models using eqn (4) and (5) respectively.

$$\frac{C_e}{Q_e} = \frac{1}{Q_m K_L} + \frac{1}{Q_m} C_e \quad (4)$$

$$\ln Q_e = \ln K_F + \frac{1}{n} \ln C_e \quad (5)$$

Here Q_e (mg g^{-1}) is the equilibrium adsorption capacity and Q_m (mg g^{-1}) is the maximum adsorption capacity. C_e is the equilibrium concentration of adsorbate (mg L^{-1}), K_L is the Langmuir constant (L mg^{-1}), and K_F is the Freundlich constant (L mg^{-1}) and $1/n$ is an indicator that reflects the nonlinear degree of adsorption.

Real-world experiments

0.25 mM solution of iodine was prepared using tap water, river water, lake water, and sea water. To 5 ml of these solutions, 10 mg of iCON-4 was added and the mixture was stirred for 3 hours. After that, the reaction mixture was filtered and the supernatant was collected for UV-vis spectroscopic analysis.

Selectivity studies

To test the selectivity of iCON-4 for iodide ions in the presence of other competing anions, 5 ml of solution containing different competing ions (such as Br^-, Cl^-, SO_4^{2-}, and NO_3^-) was prepared. Subsequently, 5 mg of the pristine iCON-4 sample was introduced into the solution. Next, the reaction mixture was filtered and the supernatant collected for UV-vis spectroscopic analysis.

K_d calculation formula

$$K_d = \left(\frac{C_0 - C_f}{C_f}\right) \times \frac{v}{m} \quad (6)$$

Using eqn (6), the values of all the distribution coefficients were calculated. Here, C_0 (mM) and C_f (mM) indicate the initial and final concentrations, respectively, whereas K_d is the distribution coefficient. Furthermore, m represents the mass of the sorbent (g), and v denotes the volume of the solution (ml).

Iodine sorption experiments in the vapor phase

In this experiment, 20 mg of iCON-4 were taken in a sealed chamber and subjected to iodine vapor exposure over 48 hours

at 75 °C and ambient pressure. In this iodine uptake experiment, initially the polymer samples were activated and introduced into a small (5 ml capacity) open vial. Next, this small vial was kept inside another larger vial (15 ml capacity) to avoid the direct contamination. Then, the larger vial (15 ml capacity) was kept inside a glass chamber with iodine granules present at the bottom. Subsequently, the glass chamber was sealed and kept in an oven at 75 °C. Periodically, the weight of the smallest vial (5 ml capacity and containing iCON-4) was recorded. A significant color change was observed in the polymeric network with the onset of iodine adsorption till the experiment ended. The iodine uptake capacities were calculated using eqn (7).

$$\alpha = \frac{m_2 - m_1}{m_1} \tag{7}$$

where α is the iodine uptake capacity in g g^{-1} and m_1 and m_2 are the weights of the vial containing iCON-4 before and after the start of the iodine vapor capture experiment. Subsequently, the data were fitted with the non-linear equations corresponding to pseudo-first order eqn (8) and pseudo-second order eqn (9) kinetics respectively.

$$Q_t = Q_e(1 - e^{-K_1 t}) \tag{8}$$

$$Q_t = \frac{K_2 Q_e^{\,2} t}{1 + K_2 Q_e t} \tag{9}$$

where Q_t (g g^{-1}) and Q_e (g g^{-1}) are the amounts of sorbate captured by iCON-4 at different time intervals (t) and at equilibrium respectively. Herein, t represents the time in hours, and k_1 ($hour^{-1}$) and K_2 (g g^{-1} h^{-1}) are the rate constants for pseudo first-order and pseudo-second order reactions.

Iodine release and adsorbent (iCON-4) regeneration by heating

20 mg of iodine-adsorbed polymer (I_2@iCON-4) was placed in an open glass vial and heated on a sand bath at 125 °C and 1.0 bar. The iodine release efficiency (R_e) was calculated from the recorded weight losses in the sample of I_2@iCON-4 using eqn (10):

$$R_e = \frac{(20 - M_t)}{M_x} \times 100\% \tag{10}$$

where M_t is the weight of the polymer after time t (t ranges from 0 to 300 min) and M_x is the weight of iodine captured in 20 mg I_2@iCON-4.

Iodine release and adsorbent (iCON-4) regeneration by extraction in MeOH

The release of iodine from I_2@iCON-4 was also performed by using methanol. In these experiments, 5 mg of I_2@iCON-4 was weighed and placed in a 20 ml glass vial. 15 ml of methanol was then added, and at predetermined time intervals, the UV-vis spectra of the methanol aliquots were recorded. The color of methanol gradually changed from colorless to yellowish-brown, indicating the release of iodine from I_2@iCON-4. The release of polyiodide ions into the solution was indicated by an increase in the absorbance of the peaks with an absorption maximum at 290 and 358 nm.

Characterization

The Fourier transform infrared (FTIR) spectra of samples were recorded using a PerkinElmer 400 FTIR spectrophotometer in the range of 500–4000 cm^{-1}. Solid-state ^{13}C CP-MAS NMR spectra were recorded using a 400 MHz Bruker NMR instrument. The powder X-ray diffraction (PXRD) patterns of iCON-4 were obtained using a PANalytical X-ray diffractometer using Cu Kα radiation (α = 1.5406 Å), with a range of 5° to 50° and a scan speed of 2° min^{-1}. Thermogravimetric analysis (TGA) of iCON-4 was carried out using a PerkinElmer STA 6000 analyser. The sample was heated in the temperature range of 30–700 °C under a nitrogen atmosphere. The heating rate in the TGA experiment was set at 10 °C min^{-1}. The surface area and porous properties of iCON-4 were estimated using a Quantachrome Autosorb iQ2 instrument (Quantachrome, USA) and extra-high purity gases. Before analysis, iCON-4 was heated at 120 °C overnight to activate it. Subsequently, the sample was subjected to nitrogen gas adsorption (P/P_0 range from 0 to 1 atm) measurements at 77 K. Gas uptake and pore size data were analysed by using the Quantachrome ASiQwin Version 3.01 software provided with the instrument. In addition, the specific surface area of iCON-4 was calculated by using the Brunauer–Emmett–Teller (BET) model. Furthermore, the pore size distribution was obtained from the sorption curves by employing non-local density functional theory (NLDFT). An Anton Paar Litesizer 500 was used to estimate the zeta-potential value of iCON-4 with 100 runs (in the manual mode). FESEM micrographs were recorded using a ZEISS Field Emission Scanning Electron Microscope (FESEM). Prior to SEM analysis, the samples were sputter-coated with gold. Also, to perform the elemental analyses, a voltage of 20 kV was applied using an EDX (Energy dispersive X-ray) detector. UV-visible absorption spectra were monitored on a Shimadzu UV-2550 UV-vis spectrophotometer to study the capture of iodine from both aqueous and vapor media. The Raman spectra were recorded with a 514 nm laser with an exposure time of 10 s by utilizing a Micro-Raman spectrophotometer (STR 750 RAMAN spectrograph, Seki Technotron Corporation Japan). All the digital images being reported herein were captured using a Motorola moto g60 mobile camera.

Results and discussion

Schiff base polycondensation is a facile, efficient, and simple synthetic route to obtain porous polymeric materials with covalent linkages. However, the use of acid/metal catalysts in Schiff base reactions is very common. In this regard, we have employed a 'greener approach' to synthesize a unique ionic covalent organic network (iCON-4) containing imine linkages. In the polymerization reaction, a water/dioxane mixture was used as a solvent/reaction medium. Terephthalaldehyde (TP) and triaminoguanidinium chloride (TAG_{Cl}) were used as monomers to the form the desired iCON-4 as a bright-yellow solid precipitate (iCON-4) that was washed with copious quantities of tetrahydrofuran (THF), ethanol, DMF, and water. The polymer was further purified by using a Soxhlet extractor containing methanol and THF. The obtained product was dried for

24 h by placing it in a vacuum oven at around 90 °C. The pristine polymer (iCON-4) thus obtained was characterized using techniques commonly used for porous organic polymers.

Specifically, iCON-4 was characterized using Fourier transform infrared (FTIR) spectroscopy, ^{13}C solid-state CP-MAS NMR spectroscopy, powder X-ray diffraction (PXRD), low temperature (77 K) nitrogen gas adsorption, thermogravimetric analysis (TGA), field emission scanning electron microscopy (FESEM) and energy dispersive X-ray (EDX) analysis. FTIR was used to confirm the formation of covalent linkages between both the monomers in the obtained product. As illustrated in Fig. 1a, the bands centered at 3310 cm $^{-1}$ and 3182 cm^{-1} in the IR spectrum of monomer TAG_{Cl} were related to the presence of $-NH_2$ moieties. On the other hand, a strong and sharp band at 1690 cm^{-1} was recorded in the IR spectrum of TP that was assigned to the –C═O stretching vibration in this monomer (TP). However, in the spectrum of the polymerised product (iCON-4), the characteristic peaks of the monomers (TAG_{Cl} and TP) were absent, indicating the complete reaction of both aldehyde and amine functional groups. Furthermore, a new band centered at 1614 cm^{-1} was observed in the IR spectrum of iCON-4 that was attributed to the presence of abundant –C═N– bonds. This clearly demonstrated the successful polymerization of TAG_{Cl} and TP *via* formation of imine linkages.[66] Since the polymer is not soluble in any common organic solvents (Table S1†), solid-state ^{13}C CP MAS NMR spectroscopy was used to study the carbon environment of iCON-4. As shown in Fig. 1b, broad peaks centered at δ 148.41 ppm indicated the presence of abundant imine (–C═N–) units in iCON-4. The peak present at 151.04 ppm is due the presence of carbon of the guanidium unit. The signals observed in the range 140 to 120 ppm are due to the carbon atoms of the arene rings present in iCON-4.[67] To assess the crystallinity of iCON-4, a powder X-ray diffraction experiment was performed. The absence of any strong diffraction peak in the PXRD spectra revealed the non-crystalline nature of iCON-4(Fig. 1c). The broad peak observed between 20 and 30 (2θ) degrees is probably due to the π–π stacking interactions of arene moieties present in iCON-4.

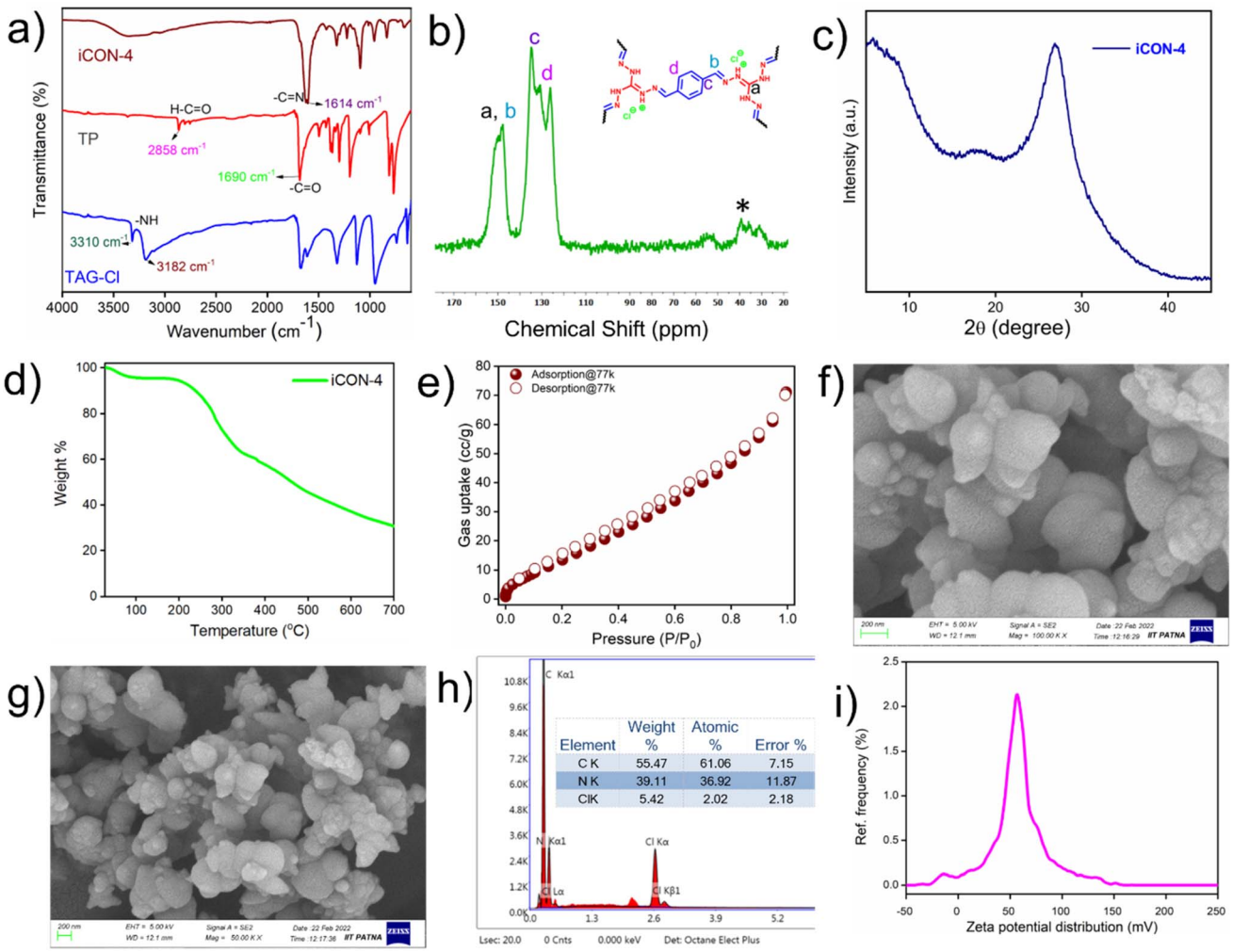

Fig. 1 Structural characterization of iCON-4: (a) FTIR spectrum of iCON-4 compared with that of the monomers, (b) solid-state ^{13}C CP-MAS NMR spectrum of iCON-4, (c) PXRD pattern of iCON-4, (d) TGA analysis of iCON-4, (e) N_2 gas adsorption and desorption curves of iCON-4 recorded at 77 K, (f and g) FESEM images of iCON-4 at different magnifications, (h) EDX analysis of iCON-4, and (i) zeta potential plot of iCON-4.

Furthermore, to comment on the thermal stability of iCON-4, thermogravimetric analysis (TGA) of its pristine sample was performed. The experiment was carried out in a nitrogen environment within temperatures ranging from 30 °C to 700 °C. The initial weight loss observed in the TGA thermogram (Fig. 1d) of iCON-4 was due to the removal of solvent molecules from the pores of the ionic network. Furthermore, weight losses at temperatures greater than 200 °C were due to slow degradation of iCON-4.[68]

The porosity and specific surface area parameters of iCON-4 were investigated by recording nitrogen adsorption and desorption isotherms at the boiling point of liquid N_2 (Fig. 1e). The surface area of iCON-4 was calculated using the Brunauer–Emmett–Teller (BET) method, and it was found to be 30.55 m^2 g^{-1}. The observed low BET surface area was due to the availability of chloride counter anions present inside the pores and surface leading to consequent reduction of the available void space to a significant extent.[66] The pore volume and pore diameter parameters, studied using the NLDFT (non-local density functional theory) method (Fig. S1†), were found to be 0.064 cm^3 g^{-1} and 1.45 nm respectively. Furthermore, to gain insight into the morphology of iCON-4, field emission scanning electron microscope (FESEM) images were captured. The FESEM micrographs were taken at different magnifications and they are shown in Fig. 1f and g. The SEM pictures of iCON-4 indicated the presence of nanodimensional and polydispersed agglomerates whose dimensions range from tens of nanometers to a few hundreds of nanometers. SEM-EDX analysis confirmed that iCON-4 contains trapped chloride anions (Fig. 1h). The surface charge distribution of iCON-4 was estimated by measuring the zeta potential (Fig. 1i). The corresponding value of +79.45 mV implied the presence of a strong positive charge distribution on the surface of the polymeric network (iCON-4). In order to investigate the chemical stability of iCON-4, a few milligrams of the compound were soaked separately in HCl and NaOH solutions. After 3 days of soaking, the obtained iCON-4 samples were separated by filtration and further characterized by FTIR spectroscopy. The FTIR spectra (Fig. S2†) of the acid/base treated samples were found to be similar to that of the pristine one. This clearly led us to conclude that iCON-4 is a robust material with good chemical stability under both acidic and basic conditions.

The availability of plenty of nitrogen centres and an electron-rich π-environment in the polymeric network of iCON-4 intrigued us to study its iodine adsorption capacity from various aqueous media. Moreover, considering that iCON-4 is a cationic network with abundant polar sites, it had substantial potential to act as an adsorbent for anionic species of iodine present in aqueous samples.[61,69] It was anticipated that during the course of capture of anionic iodine species, the chloride ions might be replaced by I_3^- anions through an ion-exchange based adsorption mechanism. We studied the potential of iCON-4 to capture I_3^- ions from its aqueous solution by using a UV-vis spectrophotometer. In these experiments, a weighed sample of iCON-4 was soaked in a 0.25 mM iodine solution to calculate the adsorption kinetics of iCON-4 (Fig. 2a). Within

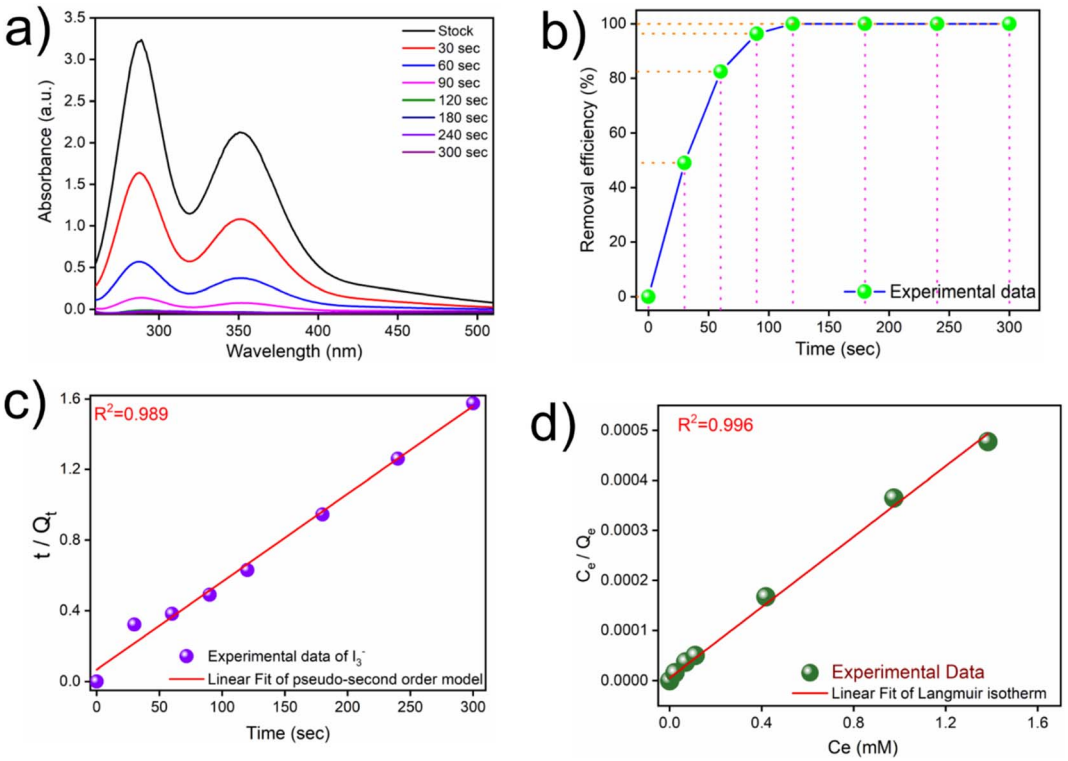

Fig. 2 (a) UV-vis spectra of iodine capture from aqueous solutions by iCON-4 at different time intervals, (b) extent of iodine captured by iCON-4 from aqueous solutions at various time intervals, (c) linear fitting of data to a pseudo-second order model, and (d) linear fitting of data (I_3^- uptake by iCON-4) to the Langmuir model.

a few minutes, the color of the solution changed from dark yellow to nearly colorless, whereas the color of particles transformed from yellow to almost black. The concentration of iodine decreased rapidly with the passage of time and it became close to 0.01 mM in approximately 120 seconds (Fig. S3†). Specifically, iCON-4 removed almost 99% of polyiodide ions in 120 seconds (Fig. 2b) from aqueous solution. Thus, iCON-4 demonstrated ultrafast kinetics for the removal of iodine species from aqueous solutions, which is desirable in an efficient sorbent. Such fast kinetics is higher than those in the previously reported literature and a comparison table is illustrated in Table S2.† The experimental data were fitted using pseudo-first order (Fig. S4†) and pseudo-second order kinetic models (Fig. 2c).

The correlation coefficient value (R^2) of pseudo-second order was relatively higher than that for pseudo-first order, which indicated that the iodine species adsorption mechanism by iCON-4 may be obeying a pseudo-second order kinetic model. Furthermore, to understand the interaction between iCON-4 and iodine, adsorption isotherm studies were performed. The Freundlich adsorption model is applicable for multilayer adsorption occurring on the heterogeneous surface, while the Langmuir model assumes monolayer adsorption on the homogeneous surface. The adsorption isotherms were recorded using 10 mg of iCON-4 suspended in 5 ml of iodine solution of varying concentrations. Subsequently, the data obtained from the adsorption isotherm were fitted with both Langmuir (Fig. 2d) and Freundlich isotherm models (Fig. S5†). The data had a better fit with the Langmuir model (with a higher regression coefficient value greater than 0.99) in comparison to the Freundlich model. In addition, the highest adsorption capacity recorded by iCON-4 was found to be 1632.17 mg g^{-1}, which is similar to or even greater than that of most of the adsorbents reported to date (Table S3†). A column adsorption experiment was also carried out in order to indicate the removal of polyiodide ions from the aqueous solution (Fig. S6†). A glass column of length 20 cm and diameter 0.5 cm was used in the experiment. The flow rate of eluent was found to be approximately 2 ml min^{-1}. The length of the adsorbent packed in the column was approximately 2.5 cm. A 25 ml solution of I_3^- (0.25 mM) was passed through the column entirely and the eluent was collected as a single fraction that was tested for the presence of iodide species using UV-vis spectroscopy (Fig. 3a). Furthermore, we evaluated the values of the distribution coefficient (K_d) associated with I_3^- capture.

Generally, the K_d values denote the affinity of an adsorbent material towards the adsorbate, and magnitudes of K_d greater than 10^4 ml g^{-1} are considered as exceptional.[70] For iCON-4, the value of K_d was determined to be in the order of 10^5 ml g^{-1} which suggests exceptionally high affinity of this sorbent towards I_3^- ions.[71] Since the rate of iodine capture from an aqueous medium by iCON-4 was very fast, we were curious to probe the material's potential to capture iodine from real-time aqueous samples. Also, the United States Environmental Protection Agency (US-EPA) suggested iodine as an urgent biocide for drinking water.[70] In this regard, we have performed iodine capture experiments in natural water resources such as sea water, river water, lake water, and tap water. Again, the removal of iodine was analysed using a UV-vis spectrophotometer (Fig. S7 and S8†). Within 5 minutes, iCON-4 removed iodine almost quantitatively from all above aqueous samples (Fig. 3b). The above experimental results suggest that iCON-4 might be useful as an adsorbent for practical applications, while extracting radioiodine pollutants that might be present in various water bodies. In aqueous solution, iodine may exist as either neutral molecular iodine (I_2) or anionic triiodide (I_3^-), which are obtained by combination of I_2 and I^- ($I_2 + I^- \rightleftharpoons I_3^-$ equilibrium). Based upon the data obtained from kinetic and adsorption studies, the plausible mechanism of capture of iodine species is *via* an ion-exchange mechanism in which chloride ions are rapidly exchanged by anionic iodine species such as I^- or I_3^-.[71,72] Furthermore, we have investigated the ability of iCON-4 to selectively capture iodine species in the presence of other anionic species as is desired for a solid adsorbent intended for application in real-time scenarios. Typically, contaminated water may contain several competing anionic species such as sulphate (SO_4^{2-}), bromide (Br^-), nitrate (NO_3^-) and chloride (Cl^-) that may retard or even hinder the efficient iodine species uptake shown by iCON-4. In this context, aqueous solutions of a binary mixture of anions containing an equimolar amount of I_3^- and another competing ion (such as SO_4^{2-}, Br^-, NO_3^- and Cl^-) were prepared and a weighed quantity of iCON-4 was suspended in it. No significant deterioration in I_3^- removal performance was observed in the

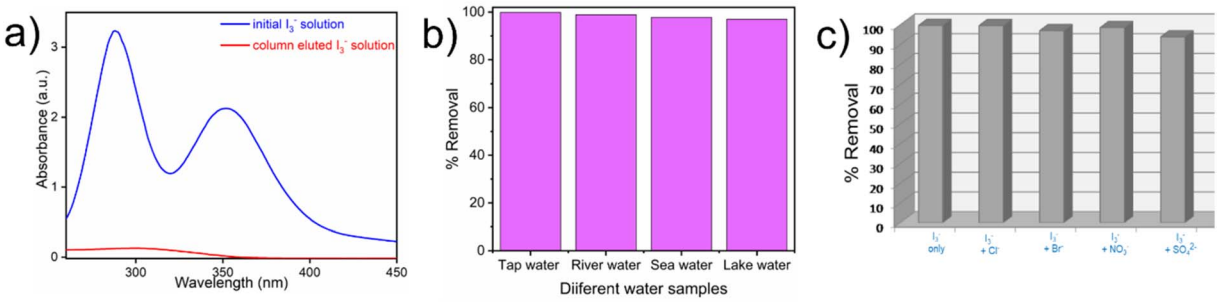

Fig. 3 (a) Column based I_3^- removal with 25 ml of 0.25 mM I_3^- solution, (b) I_3^- uptake from water samples collected from different sources, and (c) selective uptake of I_3^- ions in the presence of different interfering anions.

presence of other competing anions. Additionally, we investigated the performance of iCON-4 for iodine in a specific water sample when multiple competing anions (SO_4^{2-}, Br^-, NO_3^- and Cl^-) are present. Still, iCON-4 exhibited good uptake capacity similar to that observed in solutions containing a binary mixture of anions (Fig. 3c). Additionally, we have explored the application of iCON-4 as an adsorbent of pure iodine dissolved in water. In this experiment, first we have prepared 1 mM I_2 solution in water. The uptake capacity was calculated from the UV-vis spectra and the maximum capture capacity was obtained as 1134 mg g^{-1} (Fig. S9†).[73] Also, an iodine adsorption experiment was performed from *n*-hexane solution. Using a 5 mM I_2 solution, the maximum capture capacity shown by iCON-4 was 1014 mg g^{-1} (Fig. S10†).

Next, a sample of iCON-4 was explored for its ability to capture iodine present in the vapor phase. Data related to gravimetric measurements are shown in Fig. 4a wherein the iCON-4 sample was exposed to I_2 vapors at 75 °C and ambient pressure for 48 h.[74,75] These experimental conditions simulate the conditions required for reprocessing of nuclear fuels. A vial-in-vial setup was employed to assess iodine uptake in the vapor phase using the ^{127}I isotope with chemical properties similar to those of radioiodine isotopes (such as ^{129}I and ^{131}I).

The iodine capture capacity of the iCON-4 sample was monitored at regular intervals of time. It was found that the uptake capacity was fast during the first 24 h of the experiment, and after that the uptake rate decreased gradually. The data suggest that the equilibrium was established within 40 h and subsequently, the increase in the weight of the sample was not significant. The highest equilibrium iodine uptake capacity of iCON-4 was recorded at 5735 mg g^{-1}. This is one of the highest uptake values among porous organic polymers reported to date. The kinetics of iodine vapor capture (Fig. 4b) was also studied and results indicate that the gravimetric iodine capture by iCON-4 followed pseudo-second order kinetics.

The ability of an adsorbent to retain the adsorbate is an important parameter. Therefore, the retention capacity of iCON-4 was studied in which an I_2@iCON-4 sample was exposed to air under atmospheric conditions and its weight loss (if any) was measured at different time intervals. It was observed that there was no substantial weight loss of the sample over a period of several days, indicating the excellent iodine retention capacity of iCON-4 (Fig. S11†).

To propose a possible mechanism of iodine capture by iCON-4, the samples of I_2@iCON-4 and iCON-4 were compared using the FTIR spectra, Raman spectra, FESEM, EDX and TGA. In FTIR spectra (Fig. 5a), there was a shift in the position of the characteristic bands of I_2@iCON-4 as compared to those in the spectrum of iCON-4. For example, after iodine uptake by iCON-4, the band due the –C=N stretching shifted from 1572 cm^{-1} to 1563 cm^{-1} while the band due to –C–N stretching shifted from 1208 cm^{-1} to 1200 cm^{-1}. The observed changes in the FTIR-spectra implied that the nitrogen centres were instrumental as binding centres for iodine molecules. Moreover, the minor repositioning of other bands indicated the presence of weak interactions leading to the physisorption of iodine molecules on the surface of iCON-4. On comparing the FESEM images of pristine and iodine-loaded iCON-4 (Fig. 5b and c), significant morphological changes were observed. The growth of very small aggregates can be seen in I_2@iCON-4, which were absent in the micrographs of the pristine polymer, suggesting the accumulation of I_2 on the relatively smooth texture of iCON-4. In addition, the EDX analysis of a specimen of I_2@iCON-4 showed a high iodine content as indicated in Fig. 5d and e. A TGA analysis of I_2@iCON-4 was performed which showed a significantly higher weight loss relative to pristine iCON-4 in the temperature range of 70–400 °C, attributed to the release of adsorbed iodine from I_2@iCON-4 (Fig. 5f). The nature of iodine species presents in I_2@iCON-4 was investigated by Raman spectroscopy (Fig. 5g). Due to the lack of any iodine species, the corresponding peaks were not detected in the Raman spectra of pristine iCON-4. However, a highly intense peak was observed at 167 cm^{-1} in a sample of I_2@iCON-4, which indicated the existence of iodine as a polyiodide species.[76] The aqueous phase iodine capture is mostly governed by an ion exchange based adsorption mechanism as illustrated in Fig. 6.

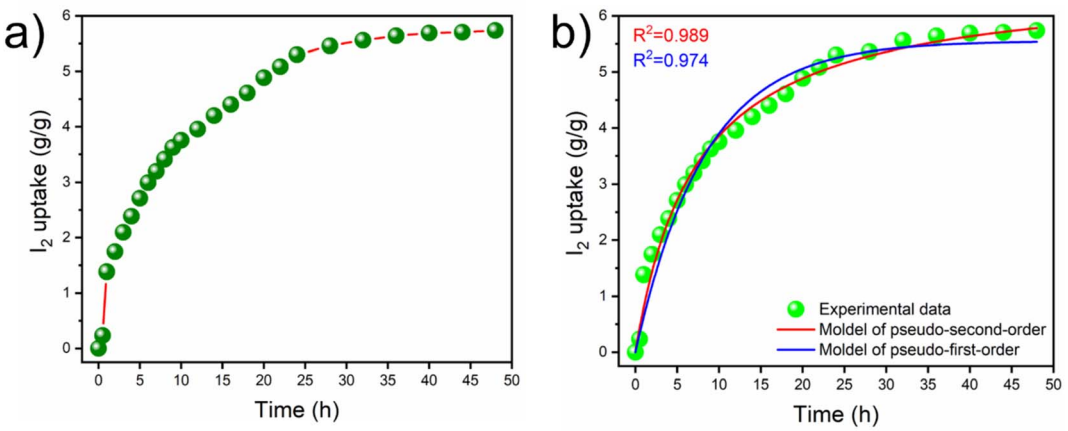

Fig. 4 (a) Curve depicting iodine vapor uptake by iCON-4 at 75 °C and (b) non-linear fitting of iodine vapor uptake (by iCON-4) data to pseudo-first and pseudo second order kinetics.

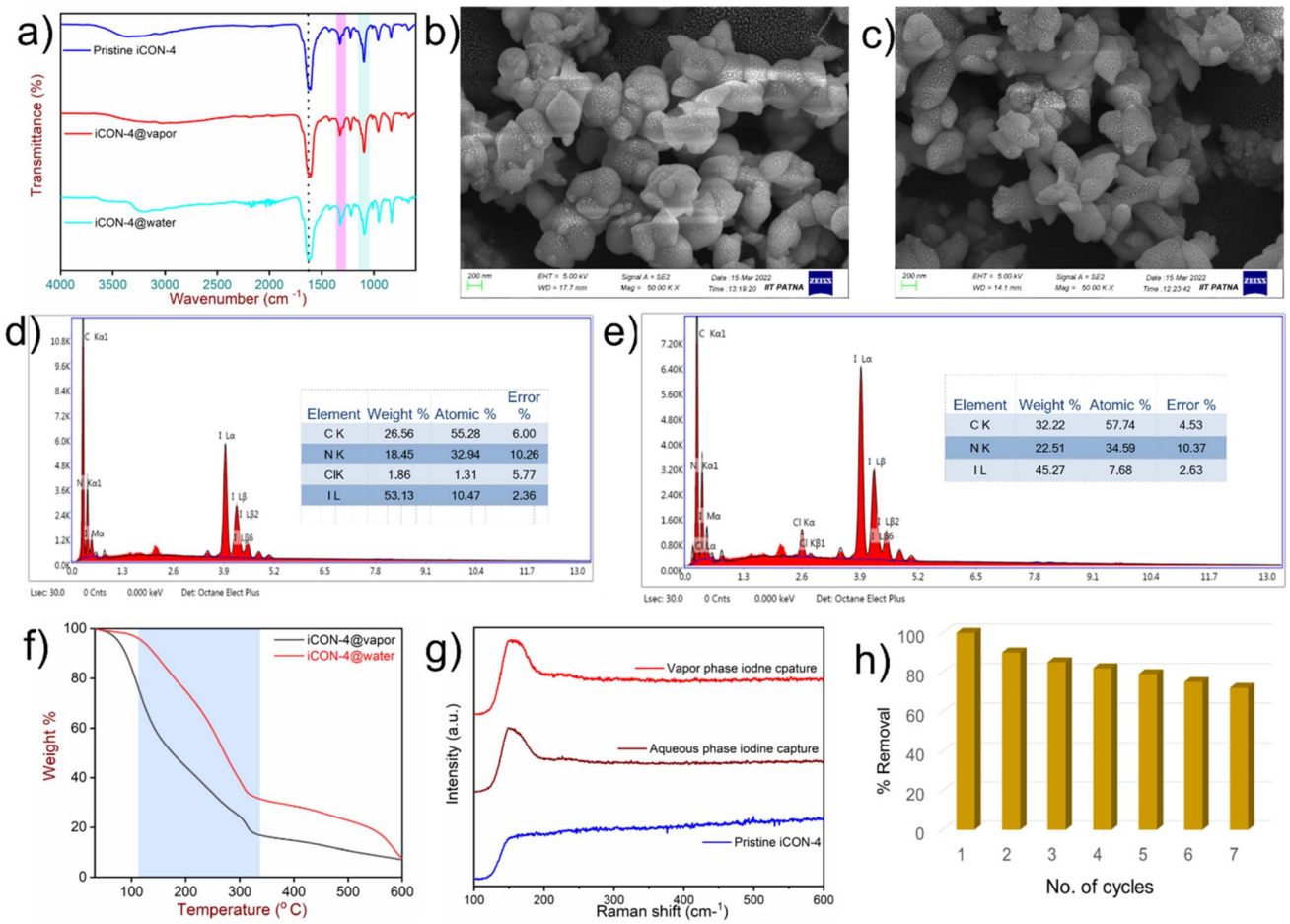

Fig. 5 (a) FTIR spectra of pristine iCON-4 and post capture of iodine [iCON-4@vapor and iCON-4@water] from various media, (b) FESEM image of I_2@iCON-4 obtained after capture of iodine vapors, (c) FESEM image of I_2@iCON-4 obtained after capture of iodide anions dissolved in water, (d) EDX analysis of I_2@iCON-4 obtained after capture of iodine vapors, (e) EDX analysis of I_2@iCON-4 obtained after capture of iodide anions dissolved in water, (f) post-capture TGA analysis of iCON-4@water and iCON-4@vapor, (g) Raman spectra of iCON-4 before and after iodine capture in aqueous and vapour phases, and (h) reusability of iCON-4 in the aqueous medium.

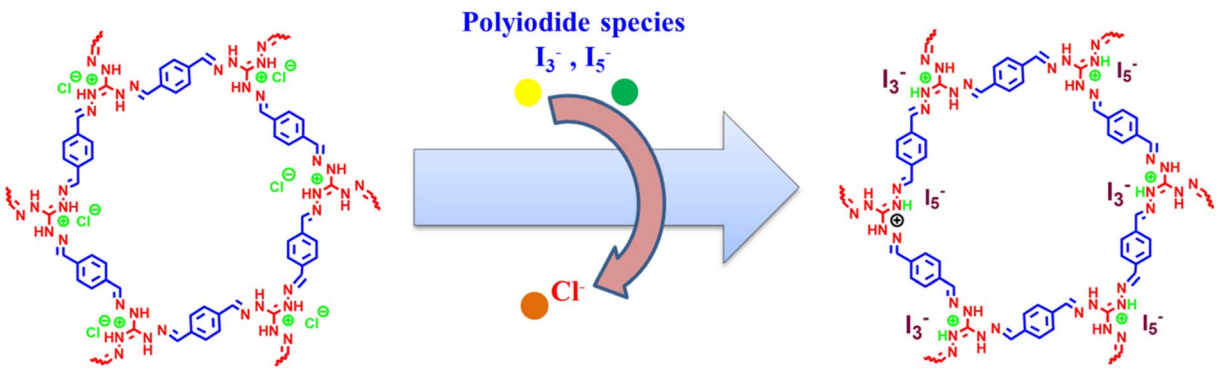

Fig. 6 Probable schematic illustration of the I_2 uptake mechanism by iCON-4 in the aqueous medium.

The results of these experiments also led us to speculate that iodine was adsorbed as I_2 *via* weak I–π interactions between iodine and benzene rings on the backbone of iCON-4 as well as stronger ion–dipole interactions between anionic I_3^- and the nitrogen centres present in iCON-4 that acted as a Lewis basic centre in the vapor phase (Fig. S12†).[77,78] It was possible to release iodine from I_2@iCON-4 by immersing the material in methanol contained in a sealed glass bottle at room temperature. With the gradual passage of time, the color of methanol changed from colorless to dark brown, indicating the release of

iodine from I_2@iCON-4. The UV-vis absorbance spectra of the methanol solution were recorded at regular intervals of time in order to quantify the iodine release. The appearance of absorbance peaks with maxima at 291 nm and 360 nm indicated the presence of polyiodide ions in methanol, which further confirmed the release of iodine species from I_2@iCON-4 samples. During the iodine desorption in methanol, the rate of adsorbate release was rapid in the first 10 minutes. Later, there was no noticeable increase in the absorbance, which led us to conclude that the desorption rate had reached equilibrium (Fig. S13†). This experiment thus verified the rapid release of iodine from I_2@iCON-4 in methanol. Furthermore, I_2@iCON-4 was regenerated by heating at 125 °C and 1.0 bar in an open glass vial on a sand bath. Approximately 85% of the adsorbed iodine was released within 30 hours as shown in Fig. S14.† Additionally, a sample of iCON-4 loaded with iodine could also be easily regenerated by immersing it in a saturated aqueous solution of sodium chloride in which rapid desorption of the adsorbed iodide anions occurred. The recyclability of an adsorbent for its multiple uses is also an important parameter while considering its cost-effectiveness. A sample of iCON-4 demonstrated negligible lowering of iodine species removal performance in the aqueous phase up to 7 cycles (Fig. 5h). This implied that iCON-4 can be reused multiple times without yielding any secondary pollutants. Furthermore, we have performed the reusability experiments of iCON-4 for iodine capture in the vapour phase. The polymer has showed minor changes in uptake capacity up to 5 cycles (Fig. S15†).

Conclusion

In summary, the facile synthesis and characterization of a guanidine-based cationic covalent organic network (iCON-4) have been described. iCON-4 is a potential adsorbent for iodine sequestration under harsh conditions usually encountered during fuel reprocessing as well as those present in polluted water samples in seas and rivers. In this context, the performance of iCON-4 as an adsorbent for iodine species was tested under challenging conditions such as highly acidic and basic environments or in the presence of competing anions in high concentration. The iCON-4 polymer exhibited high selectivity as well as stability when exposed to strongly acidic and basic pH solutions. In addition, iCON-4 showed reasonably rapid removal of iodine species from aqueous solution wherein approximately 99 percent of iodine was sequestered within 120 seconds. The isotherm model fitted according to the Langmuir model, indicating monolayer iodine adsorption with a maximum adsorption capacity of 1632.17 mg g^{-1} in water and 5735 mg g^{-1} at elevated temperatures. These performances of iCON-4 are comparable to or even better than that of other porous organic polymers reported previously in the literature (Table S3 and S4†). The facile regeneration of the iCON-4 adsorbent was possible either using a saturated aqueous solution of sodium chloride or simply immersing I_2@iCON-4 in methanol. Our results indicate that a sample of iCON-4 can be recycled easily and further used at least seven times without any significant decrease in its capture performance. The facile recyclability of iCON-4 makes it an efficient and cost-effective adsorbent for iodine removal present in various media. The capture of iodine by iCON-4 is predominantly *via* an ion-exchange mechanism in which anionic chlorides are replaced by iodides. Furthermore, the deliberate incorporation of abundant nitrogen atoms and π-rich arene rings in the polymer skeleton are responsible for the observed enhanced iodine uptake through Lewis acid–base interactions and I–π interactions respectively. We believe that our research will inspire others to synthesize newer cost-effective POPs as strategic adsorbents for efficient capture of radioactive contaminants including but not limited to radioactive iodine. This will eventually contribute towards safe use of nuclear energy and environmental remediation in the event of nuclear accidents. Ongoing research in our laboratory is on similar lines.

Conflicts of interest

The authors declare no conflicts of interest.

Acknowledgements

The authors thank the Indian Institute of Technology Patna (IIT Patna) for providing infrastructure and instrumental facilities. A. Hassan and A. Alam thankfully acknowledge IIT Patna for their respective Institute Research Fellowships. The authors acknowledge Mr S. Fajal (IISER Pune) for necessary discussions during manuscript preparation.

References

1 B. K. Sovacool, P. Schmid, A. Stirling, G. Walter and G. MacKerron, *Nat. Energy*, 2020, **5**, 928–935.
2 M. S. Dresselhaus and I. L. Thomas, *Nature*, 2001, **414**, 332–337.
3 G. Singh, J. Lee, A. Karakoti, R. Bahadur, J. Yi, D. Zhao, K. AlBahily and A. Vinu, *Chem. Soc. Rev.*, 2020, **49**, 4360–4404.
4 X. Zhang and Y. Liu, *Environ. Sci.: Nano*, 2020, **7**, 1008–1040.
5 B. K. Singh, M. A. Hafeez, H. Kim, S. Hong, J. Kang and W. Um, *ACS ES&T Eng.*, 2021, **1**, 1149–1170.
6 C. Xiao, A. Khayambashi and S. Wang, *Chem. Mater.*, 2019, **31**, 3863–3877.
7 W. Xie, D. Cui, S.-R. Zhang, Y.-H. Xu and D.-L. Jiang, *Mater. Horiz.*, 2019, **6**, 1571–1595.
8 X. Wang, L. Chen, L. Wang, Q. Fan, D. Pan, J. Li, F. Chi, Y. Xie, S. Yu, C. Xiao, F. Luo, J. Wang, X. Wang, C. Chen, W. Wu, W. Shi, S. Wang and X. Wang, *Sci. China: Chem.*, 2019, **62**, 933–967.
9 A. Hassan, A. Alam, S. Chandra, Prince and N. Das, *Environ. Sci. Adv.*, 2022, **1**, 320–330.
10 X. Hou and P. Roos, *Anal. Chim. Acta*, 2008, **608**, 105–139.
11 X. Wang, J. Xiao and G. Jiang, *Microprocess. Microsyst.*, 2021, **81**, 103660.
12 F. A. Verburg, G. Flux, L. Giovanella, D. van Nostrand, K. Muylle and M. Luster, *Eur. J. Nucl. Med. Mol. Imaging*, 2020, **47**, 78–83.

13 G. Sgouros, L. Bodei, M. R. McDevitt and J. R. Nedrow, *Nat. Rev. Drug Discovery*, 2020, **19**, 589–608.
14 J. Robbins and A. B. Schneider, *Rev. Endocr. Metab. Disord.*, 2000, **1**, 197–203.
15 J. P. Smith, S. D. Oktay, J. Kada and C. R. Olsen, *Environ. Sci. Technol.*, 2008, **42**, 5435–5440.
16 D. F. Sava, M. A. Rodriguez, K. W. Chapman, P. J. Chupas, J. A. Greathouse, P. S. Crozier and T. M. Nenoff, *J. Am. Chem. Soc.*, 2011, **133**, 12398–12401.
17 C. Muhire, A. Tesfay Reda, D. Zhang, X. Xu and C. Cui, *Chem. Eng. J.*, 2022, **431**, 133816.
18 E. D. Williams, *J. Surg. Oncol.*, 2006, **94**, 670–677.
19 World Health Organization (WHO), *Iodine as a drinking-water disinfectant*, Switzerland, 2018.
20 H. Backer and J. Hollowell, *Environ. Health Perspect.*, 2000, **108**, 679–684.
21 L. F. Diaz, G. M. Savage and L. L. Eggerth, *Waste Manage.*, 2005, **25**, 626–637.
22 X. Zhang, J. Maddock, T. M. Nenoff, M. A. Denecke, S. Yang and M. Schröder, *Chem. Soc. Rev.*, 2022, **51**, 3243–3262.
23 Y.-N. Yu, Z. Yin, L.-H. Cao and Y.-M. Ma, *J. Inclusion Phenom. Macrocyclic Chem.*, 2022, **102**, 395–427.
24 S.-T. Wang, Y.-J. Liu, C.-Y. Zhang, F. Yang, W.-H. Fang and J. Zhang, *Chem.–Eur. J.*, 2023, **29**, e202202638.
25 B. J. Riley, J. D. Vienna, D. M. Strachan, J. S. McCloy and J. L. Jerden, *J. Nucl. Mater.*, 2016, **470**, 307–326.
26 T. J. Robshaw, J. Turner, S. Kearney, B. Walkley, C. A. Sharrad and M. D. Ogden, *SN Appl. Sci.*, 2021, **3**, 843.
27 E. D. Miensah, A. Gu, L. T. Kokuloku Jr, K. Chen, P. Wang, C. Gong, P. Mao, K. Chen, Y. Jiao and Y. Yang, *Microporous Mesoporous Mater.*, 2022, **341**, 112041.
28 A. Tesfay Reda, M. Pan, D. Zhang and X. Xu, *J. Environ. Chem. Eng.*, 2021, **9**, 105279.
29 T. Skorjanc, D. Shetty and A. Trabolsi, *Chem*, 2021, **7**, 882–918.
30 Y. Zhang, L. He, T. Pan, J. Xie, F. Wu, X. Dong, X. Wang, L. Chen, S. Gong, W. Liu, L. Kang, J. Chen, L. Chen, L. Chen, Y. Han and S. Wang, *CCS Chem.*, 2022, 1–9.
31 M. Alsalbokh, N. Fakeri, A. A. Rownaghi, D. Ludlow and F. Rezaei, *Chem. Eng. J.*, 2021, **409**, 128277.
32 N. Zhang, A. Ishag, Y. Li, H. Wang, H. Guo, P. Mei, Q. Meng and Y. Sun, *J. Cleaner Prod.*, 2020, **277**, 123360.
33 J. Huve, A. Ryzhikov, H. Nouali, V. Lalia, G. Augé and T. J. Daou, *RSC Adv.*, 2018, **8**, 29248–29273.
34 K. Umadevi and D. Mandal, *J. Environ. Radioact.*, 2021, **234**, 106623.
35 D. Luo, Y. He, J. Tian, J. L. Sessler and X. Chi, *J. Am. Chem. Soc.*, 2022, **144**, 113–117.
36 Y. Xie, T. Pan, Q. Lei, C. Chen, X. Dong, Y. Yuan, W. A. Maksoud, L. Zhao, L. Cavallo, I. Pinnau and Y. Han, *Nat. Commun.*, 2022, **13**, 2878.
37 P. Chen, X. He, M. Pang, X. Dong, S. Zhao and W. Zhang, *ACS Appl. Mater. Interfaces*, 2020, **12**, 20429–20439.
38 Y. Huang, X. Hao, S. Ma, R. Wang and Y. Wang, *Chemosphere*, 2022, **291**, 132795.
39 L. He, L. Chen, X. Dong, S. Zhang, M. Zhang, X. Dai, X. Liu, P. Lin, K. Li, C. Chen, T. Pan, F. Ma, J. Chen, M. Yuan, Y. Zhang, L. Chen, R. Zhou, Y. Han, Z. Chai and S. Wang, *Chem*, 2021, **7**, 699–714.
40 Z.-J. Li, Y. Ju, B. Yu, X. Wu, H. Lu, Y. Li, J. Zhou, X. Guo, Z.-H. Zhang, J. Lin, J.-Q. Wang and S. Wang, *Chem. Commun.*, 2020, **56**, 6715–6718.
41 A. Hassan, A. Alam, M. Ansari and N. Das, *Chem. Eng. J.*, 2022, **427**, 130950.
42 A. Hassan, S. Goswami, A. Alam, R. Bera and N. Das, *Sep. Purif. Technol.*, 2021, **257**, 117923.
43 J. Wu, F. Xu, S. Li, P. Ma, X. Zhang, Q. Liu, R. Fu and D. Wu, *Adv. Mater.*, 2019, **31**, 1802922.
44 Y. Zhu, P. Xu, X. Zhang and D. Wu, *Chem. Soc. Rev.*, 2022, **51**, 1377–1414.
45 J.-S. M. Lee and A. I. Cooper, *Chem. Rev.*, 2020, **120**, 2171–2214.
46 Q. Sun, B. Aguila, Y. Song and S. Ma, *Acc. Chem. Res.*, 2020, **53**, 812–821.
47 H. Bildirir, V. G. Gregoriou, A. Avgeropoulos, U. Scherf and C. L. Chochos, *Mater. Horiz.*, 2017, **4**, 546–556.
48 S. Wang, H. Li, H. Huang, X. Cao, X. Chen and D. Cao, *Chem. Soc. Rev.*, 2022, **51**, 2031–2080.
49 Y. Tian and G. Zhu, *Chem. Rev.*, 2020, **120**, 8934–8986.
50 Y. Xie, T. Pan, Q. Lei, C. Chen, X. Dong, Y. Yuan, J. Shen, Y. Cai, C. Zhou, I. Pinnau and Y. Han, *Angew. Chem., Int. Ed.*, 2021, **60**, 22432–22440.
51 L. Huang, R. Liu, J. Yang, Q. Shuai, B. Yuliarto, Y. V. Kaneti and Y. Yamauchi, *Chem. Eng. J.*, 2021, **408**, 127991.
52 Q. Sun, B. Aguila and S. Ma, *Trends Chem.*, 2019, **1**, 292–303.
53 S. Chandra, A. Hassan, Prince, A. Alam and N. Das, *ACS Appl. Polym. Mater.*, 2022, **4**, 6630–6641.
54 M. Sun, J. Feng, Y. Feng, X. Xin, Y. Ding and M. Sun, *TrAC, Trends Anal. Chem.*, 2022, **157**, 116829.
55 Z.-W. Liu and B.-H. Han, *Curr. Opin. Green Sustainable Chem.*, 2019, **16**, 20–25.
56 P. Zhang, Z. Wang, P. Cheng, Y. Chen and Z. Zhang, *Coord. Chem. Rev.*, 2021, **438**, 213873.
57 G. Das, B. Garai, T. Prakasam, F. Benyettou, S. Varghese, S. K. Sharma, F. Gándara, R. Pasricha, M. Baias, R. Jagannathan, N. i. Saleh, M. Elhabiri, M. A. Olson and A. Trabolsi, *Nat. Commun.*, 2022, **13**, 3904.
58 G. Das, T. Skorjanc, S. K. Sharma, F. Gándara, M. Lusi, D. S. Shankar Rao, S. Vimala, S. Krishna Prasad, J. Raya, D. S. Han, R. Jagannathan, J.-C. Olsen and A. Trabolsi, *J. Am. Chem. Soc.*, 2017, **139**, 9558–9565.
59 P. Li, J. T. Damron, V. S. Bryantsev, K. R. Johnson, D. Stamberga, S. M. Mahurin, I. Popovs and S. Jansone-Popova, *ACS Appl. Nano Mater.*, 2021, **4**, 13319–13328.
60 X. Liang, Y. Tian, Y. Yuan and Y. Kim, *Adv. Mater.*, 2021, **33**, 2105647.
61 S. Jansone-Popova, A. Moinel, J. A. Schott, S. M. Mahurin, I. Popovs, G. M. Veith and B. A. Moyer, *Environ. Sci. Technol.*, 2019, **53**, 878–883.
62 P. Blondeau, M. Segura, R. Pérez-Fernández and J. de Mendoza, *Chem. Soc. Rev.*, 2007, **36**, 198–210.
63 R. Mogaki, P. K. Hashim, K. Okuro and T. Aida, *Chem. Soc. Rev.*, 2017, **46**, 6480–6491.

64 M. Wenzel, J. Steup, K. Ohto and J. J. Weigand, *Chem. Lett.*, 2022, **51**, 20–29.
65 M. D. Best, S. L. Tobey and E. V. Anslyn, *Coord. Chem. Rev.*, 2003, **240**, 3–15.
66 S. Mitra, S. Kandambeth, B. P. Biswal, A. Khayum M, C. K. Choudhury, M. Mehta, G. Kaur, S. Banerjee, A. Prabhune, S. Verma, S. Roy, U. K. Kharul and R. Banerjee, *J. Am. Chem. Soc.*, 2016, **138**, 2823–2828.
67 P. Li, J. T. Damron, G. M. Veith, V. S. Bryantsev, S. M. Mahurin, I. Popovs and S. Jansone-Popova, *Small*, 2021, **17**, 2104703.
68 Y. Cheng, L. Zhai, M. Tong, T. Kundu, G. Liu, Y. Ying, J. Dong, Y. Wang and D. Zhao, *ACS Sustainable Chem. Eng.*, 2019, **7**, 1564–1573.
69 Z. Li, H. Li, X. Guan, J. Tang, Y. Yusran, Z. Li, M. Xue, Q. Fang, Y. Yan, V. Valtchev and S. Qiu, *J. Am. Chem. Soc.*, 2017, **139**, 17771–17774.
70 M. Zhang, J. Samanta, B. A. Atterberry, R. Staples, A. J. Rossini and C. Ke, *Angew. Chem., Int. Ed.*, 2022, **61**, e202214189; *Angew. Chem.*, 2022, **134**, e202214189.
71 A. Sen, S. Sharma, S. Dutta, M. M. Shirolkar, G. K. Dam, S. Let and S. K. Ghosh, *ACS Appl. Mater. Interfaces*, 2021, **13**, 34188–34196.
72 S. Fajal, A. Hassan, W. Mandal, M. M. Shirolkar, S. Let, N. Das and S. K. Ghosh, *Angew. Chem., Int. Ed.*, 2023, **62**, e202214095; *Angew. Chem.*, 2023, **135**, e202214095.
73 L. Xie, Z. Zheng, Q. Lin, H. Zhou, X. Ji, J. L. Sessler and H. Wang, *Angew. Chem., Int. Ed.*, 2022, **61**, e202113724.
74 Y. Zhu, Y.-J. Ji, D.-G. Wang, Y. Zhang, H. Tang, X.-R. Jia, M. Song, G. Yu and G.-C. Kuang, *J. Mater. Chem. A*, 2017, **5**, 6622–6629.
75 X. Guo, Y. Tian, M. Zhang, Y. Li, R. Wen, X. Li, X. Li, Y. Xue, L. Ma, C. Xia and S. Li, *Chem. Mater.*, 2018, **30**, 2299–2308.
76 J. Li, H. Zhang, L. Zhang, K. Wang, Z. Wang, G. Liu, Y. Zhao and Y. Zeng, *J. Mater. Chem. A*, 2020, **8**, 9523–9527.
77 P. Wang, Q. Xu, Z. Li, W. Jiang, Q. Jiang and D. Jiang, *Adv. Mater.*, 2018, **30**, 1801991.
78 S.-Y. Zhang, X.-H. Tang, Y.-L. Yan, S.-Q. Li, S. Zheng, J. Fan, X. Li, W.-G. Zhang and S. Cai, *ACS Macro Lett.*, 2021, **10**, 1590–1596.